Plasmonics
DOI 10.1007/s11468-017-0604-3

Engineering the Optical and Dielectric Properties of the Ga_2S_3/In/Ga_2S_3 Nanosandwiches via Indium Layer Thickness

Eman O. Nazzal[1,2] · **A. F. Qasrawi**[1,2,3] · **S. R. Alharbi**[1]

Received: 27 January 2017 / Accepted: 9 May 2017

Abstract In this study, the effect of the nanosandwiched indium slab thickness (20–200 nm) on the performance of the Ga_2S_3/In/Ga_2S_3 interfaces is explored by means of X-ray diffraction, Raman spectroscopy, and optical spectroscopy techniques. The indium slab thickness which was varied in the range of 20–200 nm is observed to enhance the visible light absorbability of the Ga_2S_3 by 54.6 times, engineered the energy band gap in the range of 3.7–1.4 eV and increases the dielectric constant without, significantly, altering the structure of the Ga_2S_3. The broad range of the band gap tunability and the increased absorbability nominate the Ga_2S_3 thin films for photovoltaic applications. In addition, the dielectric spectral analysis and modeling have shown that a wide variety in the plasmon resonant frequency could be established within the Ga_2S_3/In/Ga_2S_3 trilayers. The plasmon frequency engineering in the range of 0.56–2.08 GHz which is associated with drift mobility of 12.58–5.76 cm^2/Vs and electron scattering time at femtosecond level are promising for the production of broad band high frequency microwave filters.

Keywords Gallium sulfide · Optical materials · Coating · Dielectric properties · Plasmon

✉ A. F. Qasrawi
atef.qasrawi@atilim.edu.tr

[1] Department of Physics, Arab American University, Jenin, Palestine

[2] Physics Department, Faculty of Science - Al Faisaliah, King Abdulaziz University, Jeddah, Palestine

[3] Group of Physics, Faculty of Engineering, Atilim University, 06836 Ankara, Turkey

Introduction

The nanosandwiching of metal layers between two semiconducting or insulating layers has attracted the attention as a new approach to replace the particle doping [1–4]. Earlier works always considered the semiconductor or insulator (dielectric) sandwiching between two metal layers (MDM) [5]. This technique causes either ohmic or rectifying contacts to the semiconductor or insulator. Another approach of nanosandwiching gets use from two metal interfaces. It was demonstrated that the bimetal nanostructures may be employed for the engineering of the plasmonic bandwidths. The latter two approaches are viable and can be used to tune the quality factor and quantum efficiency of localized surface plasmon processes [6]. As for examples, studies on the gold nanosandwich using GeSbTe film as an active medium indicated [5] that the large difference between the extinction coefficients of the crystalline and amorphous phases of the GeSbTe enabled high-contrast switching in the magnetic dipole mode through the coupling and decoupling of Au nanorod and Au film. In another work, the nanosandwiching of the metal-dielectric-metal structure, which appeared to be promising for use as high-performance subwavelength multifunctional integrated optical devices, resulted in grating structure that can achieve extraordinary optical transmission performances at normal incidence in the ultraviolet-visible-near-infrared regions [7]. The high novel behavior of this structure was physically assigned to the metal ultraviolet transparency, surface plasmon polariton (SPP) at metal/dielectric interfaces, Fabry–Perot (FP)-like cavity mode within this dielectric grating, and optical magnetic resonance especially in the dielectric interlayer of the MDM sandwiched structure. This structure is very

Published online: 27 May 2017

important for developing high-performance subwavelength multifunctional-integrated optical devices.

On the other hand, the nanosandwiching of metal slabs between two dielectrics revealed more transparent structure that is beneficial for use in solar cell performance. The ZnS/Ag/TiO_2 multilayer, as an example, displayed a transmission coefficient of 90.23% [2]. In addition, the ZnS/Ag/ZnS nanosandwich structure displayed unique characteristics presented by low resistivity, high optical transmittance in the visible region, and high absorption in the ultraviolet regions [3]. Similarly, the studied on the ZnS/Au/ZnS indicated that an increase of Au layer thickness could result in decreasing the resistivity, increasing the carrier concentration and causes declined transmittance in the visible light region [4].

The effectiveness of the nanosandwiching technique motivated us to redesign the non-crystalline Ga_2S_3 plasmon resonators [8] via indium nanosandwiching technique. Particularly, indium thin films of various thicknesses (20–200 nm) will be inserted between two Ga_2S_3 dielectrics thin films. The changes in the structural, optical, and dielectric properties of the Ga_2S_3/In/Ga_2S_3 will be explored by the X-ray diffraction, Raman spectroscopy, and UV-VIS spectrophotometry. The dielectric dispersion is to be modeled in accordance with the existing theories. The study will allow suggesting the possible applications of these surfaces in optoelectronic technology.

Experimental Details

The 500-nm-thick Ga_2S_3 thin films are prepared by the physical deposition technique at vacuum pressure of 10^{-5} mbar from the 99.99% pure Ga_2S_3 powders (Alfa Aeser). The films were deposited onto ultrasonically cleaned glass substrates. The resulting fresh films were used as substrates to evaporate thin layers of high purity (99.999%) indium slabs of thickness of 20, 50, 100, and 200 nm. Each slab is evaporated onto separate Ga_2S_3 thin film substrate. The resulting indium-coated Ga_2S_3 films are used as substrate for the evaporation of 500-nm-thick Ga_2S_3 thin films. In all steps of deposition process, the substrate temperature was kelp at 300 K. The geometrical design of the films is shown in the inset of Fig. 1b. The nanosandwiched Ga_2S_3/In/Ga_2S_3 films were subjected to X-ray diffraction analysis using Miniflex 600 diffractometer. The data were recorded at a rate of 0.08 deg/s. The Raman spectra were recorded with the help of high resolution micro-Raman spectrometer (Thermoscientific DXR). The excitation wavelength of the Raman spectra was 532.5 nm. In addition, the optical transmittance and reflectance of the samples were recorded using Evolution 300 spectrophotometer in the incident light wavelength range of 300–1100 nm. Both of the transmittance and reflectance were recorded at normal incidence.

Results and Discussion

Owing to our previous work [8] on the energy band gap and dielectric dispersion of Ga_2S_3 thin films which revealed a direct allowed transitions energy band gap of 2.98 eV for the Ga_2S_3 films, we attempt to engineer the energy band gap of this material via nanosandwiching technique. For this purpose, indium thin films of different thicknesses of 20, 50, 100, and 200 nm were sandwiched between two layers of 500-nm-thick gallium sulfide. The resulting X-ray diffraction patterns for the four samples are displayed in Fig. 1a. As it is readable from the figure, no, remarkably, intensive peaks can be observed indicating the amorphous nature of the sandwiched films. Only one peak is observed for the sample which contains 200-nm-thick indium slabs. This peak was compared to that of In whose X-ray patterns are also displayed in the same figure. The peak in accordance to the X-ray standards (JCPDS card No.: 00-005-0642) is related to the tetragonal indium. The peaks of indium which appear in the figure were recorded for the indium which is used for the preparation of the Ga_2S_3/In/Ga_2S_3. The main reason for the non-crystalline nature of the Ga_2S_3 film could be assigned to the existence of more than one polymorph phase in the films. Namely, in its structure, the Ga_2S_3 films include the monoclinic α-Ga_2S_3, hexagonal β-Ga_2S_3, and cubic γ-Ga_2S_3 polyphases. While α phase is of ordered vacancy, the β and γ phases are of highly disordered vacancies [8, 9]. For all the samples which are sandwiched with indium slabs, as can be guessed from the broaden peak which is centered at $2\theta = 25.2°$, the enrollment of the centered tetragonal indium slab ($a = 3.25$, $c = 4.94$ Å) into the Ga_2S_3 structure does not change the physical nature of the films. The sharp small peak which also appears in the broaden peak at $2\theta = 33.2°$ is related to the indium film. The latter observation assures that the deposited films are of the same physical nature before Indium incorporation.

The Raman spectra for the Ga_2S_3/In/Ga_2S_3 interfaces are shown in Fig. 1b. As the spectrum illustrates, only one broaden very intensive peak appears at frequency of 130.6 cm^{-1} for the sample sandwiched with 20-nm indium. This peak exhibits a shoulder at 145 cm^{-1}. Increasing the indium slab thickness from 20 to 50, 100, and 200 nm shifted the active peak from 130.6 to 127.7, 126.7, and 126.7 cm^{-1}, respectively. The previously observed Raman peaks between 100 and 200 cm^{-1} were assigned to the deformation of the GaS_4 unit in the Ga_2S_3 structure [10]. The shoulders which appeared at 145 cm^{-1} are not affected by the indium thickness and were also detected in the in the Ga_2S_3-Na_2S-based glasses at 142 cm^{-1} and were attributed to the oscillation if the charge coupled cations [11]. From Fig. 1b, it is also observable that Raman peaks are broaden. The respective intensive peaks exhibit a full wave half maximum of 17.8, 19.0, 36.6, and 14.4 cm^{-1}. The broadening and shift in the active Raman

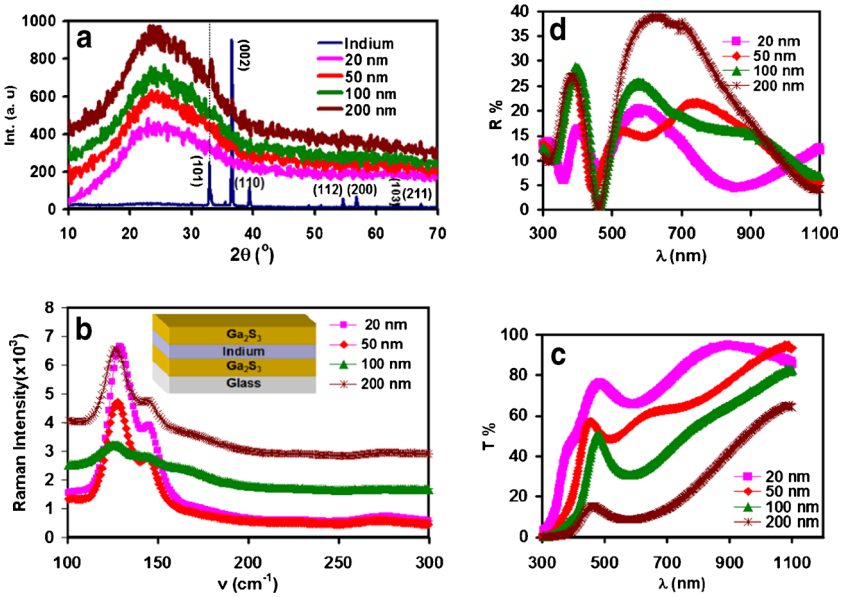

Fig. 1 **a** The X-ray diffraction, **b** the Raman spectra, **c** the transmittance spectra, and **d** the reflectance spectra for the Ga_2S_3/In/Ga_2S_3 thin films. The *inset* shows the geometrical design of the samples

frequencies of the samples arise from the lack of periodic motion beyond the unit cell dimension which in turn leads to relaxation of the zone-centre optical phonon selection rule, allowing the Raman spectrum to have additional contributions from phonons that are away from the Brillouin-zone centers [11]. Such properties of Raman spectral lines verify the amorphous nature of the films as also observed from the X-ray diffraction.

Figure 1c also displays the optical transmittance of the nanosandwiched indium films for each prepared sample. The transmittance in the films (T) decreases with increasing In slab thickness. As for example, at 900 nm, the $T\%$ values are 94.9, 77.3, 65.3, and 42.2%, for sandwiched slabs of 20, 50, 100, and 200 nm, respectively. On the other hand, the reflectance spectra which are displayed in Fig. 1d exhibit interesting features presented by two peaks that mostly appear near 400 and 580–610 nm. For the peak which appears at 400 nm, the maximum reflectivity value increases from 16% when the In slab thickness was 20 nm to ~28% when the slab thickness is increased to 200 nm. The peak which appeared near 580–610 nm exhibits characteristics that depend on the In slab thickness. Particularly, the peak maximum value is 20% at 580 nm for In sandwiching of 20 nm. It exhibits value of 26% at 580 nm for In slab thickness of 100 nm and reaches 39% at 612 nm. It is also observed that the reflectance shows a minima at 460 nm for In layer thickness of 20, 100, and 200 nm and at 445 nm for the 50 nm In sandwiched Ga_2S_3 films. The reflectivity of the samples at these positions sharply falls to zero as the In layer thickness increases to 100 and 200 nm. The explanation for the existence of these peaks and their behavior will be reconsidered through the dielectric spectral analysis and modeling in this article.

The effect of the In slab thicknesses (d) on the performance of the Ga_2S_3 thin films is better screened from the absorption coefficients (α) spectra of the studied films. The absorption coefficients spectra which were calculated with the help of the equation, $T = (1-R_{Ga2S3})(1-R_{Ga2S3-In})(1-R_{Ga2S3-In-Ga2S3})\, e^{-\alpha d}/\left(1-R_{Ga2Se}R_{Ga2S3-In}R_{Ga2S3-In-Ga2S3}e^{-3\alpha d}\right)$ are displayed in Fig. 2a. The spectra displayed three different regions of absorption for the samples under investigation: the high absorption region (4.0–3.3 eV), the moderate region (3.3–2.6 eV), and the low absorption region (2.6–1.2 eV). In all regions, the absorption coefficient values increase with increasing indium slab thickness. As for example, at 3.5 eV, the absorption coefficient value increases from $1.44\times10^4(cm^{-1})$ to $2.40\times10^4(cm^{-1})$ and reaches $3.85\times10^4(cm^{-1})$ when the slab thickness increases from 20 to 50 and reaches 200 nm. The ratios of the absorption coefficients of the sandwiched films to those which were deposited without In sandwiching (previously reported in ref. [8]) $R_\alpha = \frac{\alpha(Ga_2S_3/In/Ga_2S_3)}{\alpha(Ga_2S_3)}$ are presented in Fig. 2b. The $R_\lambda - E$ dependencies display three peaks at 3.10, 2.34, and 1.21 eV. At these three energy positions, the indium slab effect is clearly pronounced. Particularly, while the absorbance increased by 6.0 times when the slab thickness reaches 200 nm at 3.10 eV, R_λ exhibits values of 2.5, 16.7, 20.6, and 54.6 as d exhibits values of 20, 50, 100, and 200 nm, respectively, at 2.34 eV. Similarly, one may observe a respective increase of 1.1, 2.0, 11.5, and 38.1 at 1.21 eV. The enhanced absorbability of light spectra at 2.34 eV is highly promising as it indicates remarkable optical engineering of the Ga_2S_3 by the nanosandwiching method.

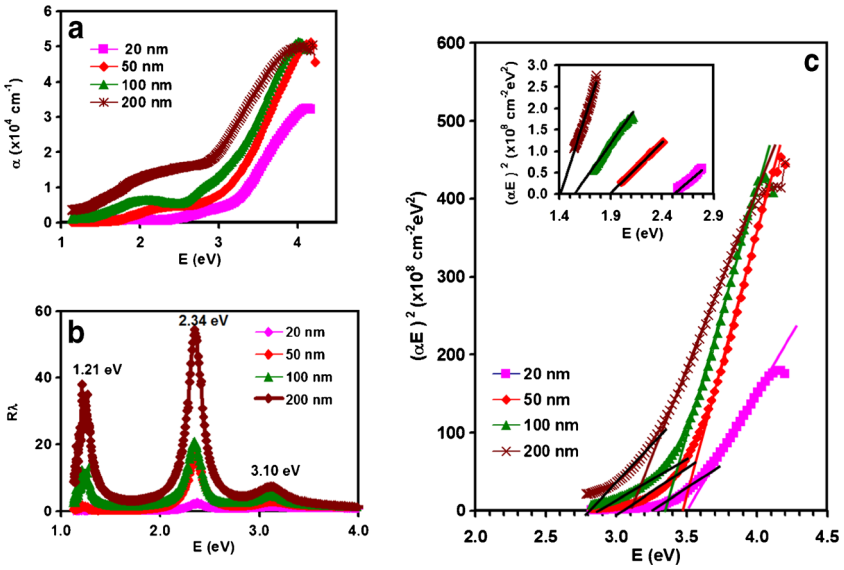

Fig. 2 **a** The absorption coefficient spectra, **b** the absorbability of the In nanosandwiched Ga_2S_3, and **c** the $(\alpha E)^2 - E$ dependence of the Ga_2S_3/In/Ga_2S_3 interface in the high and moderate absorption regions. The *inset* of (**c**) shows the $(\alpha E)^2 - E$ dependence in the low absorption region

The spectral data are displayed in Fig. 2c and its inset represents the Tauc [8] method for energy band gap estimation. The $E-axis$ crossing of the $(\alpha E)^2 - E$ variations reveals information about the direct allowed transitions energy band gap of the nanosandwiched films in the three absorption regions. The solid lines which are shown in the figure cross the $E-axis$ at the energy position which is shown in Table 1. The figure and the table illustrate large shift in the energy band gap value as a response to the increases in the sandwiched indium slab. In the high absorption region, the energy band gap decreases from 3.68 eV for pure Ga_2S_3 to 3.50 eV and reaches 3.10 eV as the indium slab thickness increases from 20 nm and reaches 200 nm. It indicates a band gap tuning of 0.58 eV in the blue light region. In the moderate absorption region, the energy band gap increased from 2.98 eV for samples which contain no indium slab to 3.25 eV as the indium slab exhibits thickness of 20 nm and decreases to 2.80 as the thickness of the slab reaches 200 nm. In the moderate absorption region, the energy shifts from dark to light blue limit. It indicates less sensitivity to the metal insertion between the two dielectric films. On the other hand, in the third absorption region (2.6–1.2 eV), the energy band gap lowers from 2.51 eV in the absence of the slab to 1.89 eV as the indium slab thickness reaches 50 nm. It also exhibits value of 1.41 eV for 200-nm-thick nanosandwiched indium. The tunability in this range of light is very high (1.10 eV). It indicates a shift from light blue to the near infrared region. This range, approximately, covers all the visible range of light. That wide range of tunability gains importance because it covers most of the sun spectra and with the high absorption property the Ga_2S_3/In/Ga_2S_3 interface turn out to be promising candidate for solar cell production as well as other optoelectronic applications.

Table 1 The energy band gap the Ga_2S_3/In/Ga_2S_3 interface at various thicknesses

Thickness (nm)	E_{g1} (eV)	E_{g2} (eV)	E_{g3} (eV)
0	3.68	2.98	2.51
20	3.50	3.25	2.50
50	3.48	3.12	1.89
100	3.34	2.90	1.55
200	3.10	2.80	1.41

Literature data indicated an energy band gap value of ~3.44 eV for the monoclinic structured α–Ga_2S_3 (wurtzite). This polyphase of the gallium sulfide is reported to exhibit ordered vacancy with lattice parameters of a = 11.094, b = 9.578, c = 6.395 Å, and γ=141° 15′ [8–12]. In addition, both of the β–Ga_2S_3 (wurtzite type) polyphase and γ–Ga_2S_3 (zincblende type) phase are known to have high disordered vacancy in its respective hexagonal (lattice parameters of a = 3.678 and c = 6.395 Å) and cubic (5.441 Å) structures. The energy band gap for the β–Ga_2S_3 is 2.48 eV and that of γ–Ga_2S_3 is ~3.0 eV [8–12]. On the other hand, the temperature dependent photoluminescence studies on GaS crystal revealed the existence of three energy bands known as A, B, and C with respective band gap energies of 2.2, 2.02, and 1.59 eV [13]. The existence of these energy bands was ascribed to the donor–acceptor pair recombination processes in gallium sulfide [13]. The recombination centers are reported to be located at the nearest neighbor lattice or interstitial site. Both of the gallium vacancies with different charge states and sulfur interstitial can effectively be involved in electronic transitions.

Our X-ray diffraction (Fig. 1a) data and our current and early published energy dispersion X-ray (EDX) analysis [8] revealed the amorphous nature of the films and the physical nature of deposition. The physical nature of deposition which was tested by the EDX onto metals like gold and

semiconducting substrates like (p–Ge and n–InSe) revealed a stoichiometric composition of Ga_2S_3 with atomic content of $Ga_{41}S_{59}$ when deposited onto metals and semiconductor substrates. Some regions near the edge of the films were observed to exhibit the atomic content of $Ga_{49}S_{51}$. Thus, mostly, the morphology is ascribed to the existence of more than polymorphic phase of Ga_2S_3 in the structure of the thin films rather than the non-stoichiometric distribution [8–13]. This is also confirmed from the optical absorption coefficient spectral analysis where three energy band gaps were determined from the spectral data in Fig. 2a, b. With the consideration of the random distribution of the ordered and disordered Ga vacancies through the amorphous Ga_2S_3 thin films, the understanding of the indium nanosandwiching effect on the structure of this material becomes highly complicated. The possibility of the In atom substitutions in the Ga sites should be excluded as the ionic radius of In^{+3} is 94 pm and that of Ga^{+3} is 77 pm. Still there is a possibility of interaction between the sulfur atoms near the vacant site of Gallium atom with the indium. The formation of In_2S_3 should also be considered. The In_2S_3 also exists in three polymorphic forms known as the cubic structured (a = 10.8315 Å) α–In_2S_3 which is known to exhibit spinal disordered defects due to the vacancies at the octahedral sites [14]. The tetragonal β–In_2S_3 (a = 7.623, c = 32.358 Å) exhibits an ordered spinal vacancies at the tetrahedral sites, the trigonal layered structured (a = 3.8656, c = 9.1569 Å) γ–In_2S_3 with ordered vacancy [9, 14]. The energy band gaps for α–In_2S_3, β–In_2S_3, and γ–In_2S_3 are reported to be 2.55 [15], 1.98, and 1.44 eV, respectively. The values of the energy band gap for the In_2S_3 polyphases were not detected upon evaporation of 20-nm-thick indium layers. However, when the thickness is increased to 50 nm, the low absorption region energy band gap (E_{g3}) suddenly falls from 2.50 to 1.89 eV indicating the probability of preferred electronic transitions through the In–S bonds at the indium-Ga_2S_3 interface. The average length of all possible bonding types during formation of In_2S_3 which are tabulated in ref. [16] is in the range of 2.7–2.5 Å. Those of monoclinic and cubic Ga_2S_3 are in the ranges of 2.19–2.33 and 2.25 Å, respectively [17]. The bond separation in the Ga_2S_3 is shorter than those of In_2S_3 indicating that the electronic transitions through the Ga_2S_3 may be preferred over those of In_2S_3.

From the metal-semiconductor interfacing point of view, we shall think about the ohmic/Schottky formation of the In/Ga_2S_3 interface. The electron affinity (3.30 eV [18]) and the Fermi level position below the conduction band (experimentally determined) of the n-type Ga_2S_3 reveal a work function of 3.46 eV. This value is less than the work function of the indium (4.09 [19]) indicating that a Schottky barrier of height of 0.79 eV should form at the interface between the two Ga_2S_3 layers. As a result of this Schottky barrier, an upward band bending between the upper and the lower sides of the indium slab takes place. The existence of the indium slab between the two layers of Ga_2S_3 forces the establishment of a back-to-back Schottky property in which two electric fields are brought in opposite directions on the metal sides. However, as the electron charge on the In metal sides is contained within a distance of at least one atomic layer, the charges are essentially surface charges [20, 21]. At one side, the dipole layer of charges establishes an electric field from the Ga_2S_3 to the In metal. Due to the ideal thickness of the two Ga_2S_3 layers on both sides of the metal and due to the equal and electric field density on both side of metal, we believe that the effect of Schottky barrier formation has less effect than the recombination centers on the optical performance of the Ga_2S_3/In/Ga_2S_3 nanosandwiched structures.

In a trail to clarify the reasons for the behavior of the Ga_2S_3/In/Ga_2S_3 interface upon increasing of the indium thickness, we first turn the attention to the image charges that build up in the In layer; then, as mentioned above, we consider the optical dynamics. At the In/Ga_2S_3 junction, as the carriers approach the interface region, the potential associated with these charges reduce the effective barrier height. In general, calculations of the barrier reduction assume that the charge of an electron or hole close to the metal-semiconductor interface attracts an opposite surface charge, which exactly balances the electron's (holes) charge so that the electric field surrounding the electron (holes) does not penetrate beyond this surface charge. In addition, the time to build up the surface charge and the time to polarize the Ga_2S_3 dipoles around the moving electron (hole) are assumed much shorter than the transit time of the electron [20, 21]. Since the electric field in the Ga_2S_3 is identical to that of the holes of Ga_2S_3 and electrons of In at equal distance but on the In side of the interface which is regarded as image charges, the surface charge density of the metal should be a reason for the observed energy band gap lowering. In its simplest picture, the image force depends on the square root of the electric field and on the effective dielectric constant ε_{eff} [20, 21]. While the electric field depends on the total charge density in the Ga_2S_3, where electrons, holes, ionized donors, and ionized acceptors are present, the dielectric constant depends on the externally applied electric field frequency (light in this case). Recombination of some charge carriers and accumulation of others during the interfacing process strongly affects the total surface charge density. Since the free charge of the indium resides to the surface, increasing the thickness of the indium slab necessarily indicates more freer charges on the surface that in turn attenuates the barrier height and the energy band gap as a result [20, 21].

Figure 3a displays the real part (ε_r) of the dielectric constant which was calculated from the previously given equations [8]. As seen from the figure, two main peaks may be observed in the real part of the dielectric spectra. One peak exhibits maxima near 754 THz (3.10 eV) and the other near 475 THz (1.95 eV). The two peaks are wide and separated by one minima at 650 THz (2.67 eV). The origin of these peaks

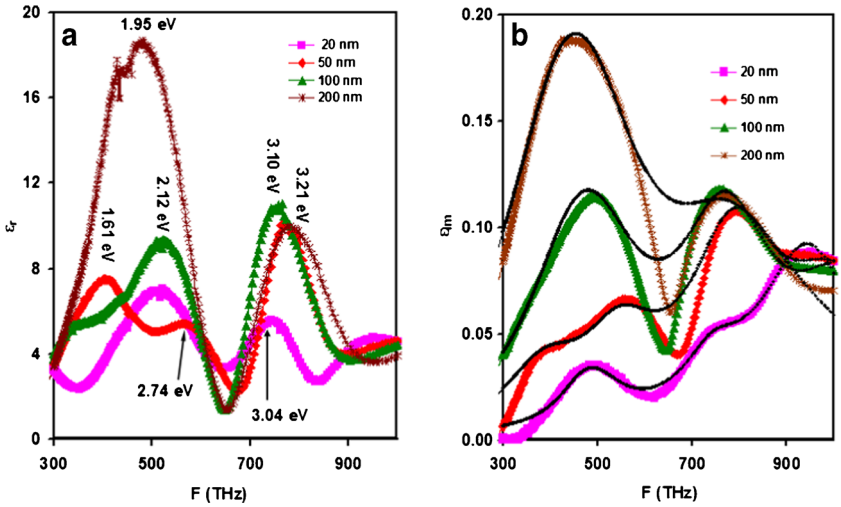

Fig. 3 **a** The real part of the dielectric spectra and **b** the imaginary part of the dielectric spectra for the Ga_2S_3/In/Ga_2S_3 interfaces at different In slab thicknesses

should be assigned to the direct transitions from the valence to the conduction band in addition to the interband transitions which arise from surface defects as previously mentioned [8]. While the valance band is constructed from sulfur (*3p*) and Ga (*4p*) orbitals, the conduction band is dominated by the Ga (*4s*) and S (*3s*) states over the range of 3.4–1.7 eV [8, 25]. In general, values of the dielectric constant show positive responsivity to the indium slab sandwiching into the Ga_2S_3 structure. As for example, at 490 THz, the dielectric constant in the absence of In slab was 3.1 [8]; it increased to 6.8 and 8.9 and reaches 18.5 as the In slab thickness increased from 20 to 100 and reaches 200 nm, respectively. A remarkable enhancement in the dielectric property of the material is observed upon In thickness increasing.

On the other hand, Fig. 3b displays the imaginary part ($\varepsilon_{\mathrm{im}}$) of the dielectric constant which also increase with increasing In slab thickness. The larger the value of the $\varepsilon_{\mathrm{im}}$,the higher the optical conductivity ($\varepsilon_{\mathrm{im}} = 4\pi\sigma/w$; σ:conductivity). Thus, the increase in the $\varepsilon_{\mathrm{im}}$ value necessarily indicates higher conductivity that probably results from the availability of more freer electrons (n) upon In thickness increasing and/or more mobile charge carriers of drift mobility ($\mu = \frac{e\tau_i}{m^*}$) in accordance with the relation, $\sigma = ne\mu$. The picture becomes clearer via Drude-Lorentz modeling for electrical conduction assuming group of coupled oscillators that follow the equation [8]:

$$\varepsilon_{\mathrm{im}} = \sum_{i=1}^{k} \frac{w_{pe_i}^2 w}{\tau_i\left(\left(w_{e_i}^2 - w^2\right)^2 + w^2\tau_i^{-2}\right)} \qquad (1)$$

The Drude–Lorentz model assumes that the electron motion is subjected to an electronic damping force of coefficient that is inversely proportional to the scattering time (τ_i). The electron cloud whose reduced resonant frequency is w_e is oscillating against ion cores of Ga^{+3}, In^{+3}, and S^{-2} causing an electron bounded plasma frequency; $w_{pe} = \sqrt{4\pi ne^2/m^*}$ ($m^* = 0.167m_o = \left(2m_{Ga2S3}^{*-1} + m_{In}^{*-1}\right)^{-1}$, $m_{In}^* = 1.02m_e$, and m_{Ga2S3}^* =0.40m_e are the effective mass of indium and Ga_2S_3, respectively [8]). The above equation reveals information about the electronic interband transitions though the assumption that the electrons in the Ga_2S_3 are bound to the ionic atomic cores (Ga^{+3}, $In^{+3,}$ and S^{-2}) and oscillate about it. The index k represents the number of oscillators at major critical points in the joint density of states which correspond to interband transition energies $\hbar w_k$, with some additional oscillators to connect absorption between critical joints [8].

The fitting of the imaginary part of the dielectric spectra is shown by solid lines in Fig. 3b. The consistency between the experimental and theoretical data was obtained through the parameters which are shown in Table 2. At particular thickness of In slabs, the scattering time decreases as the number of the oscillators (k) increases indicating that the damping force effect is more dominant at higher frequencies. In addition, an increase in the damping force coefficient (τ_i^{-1}) is observed to be associated with the increase in the nanosandwiched indium slab thickness. Particularly, the scattering time exhibits values of 1.20, 0.80, 0.65, and 0.55 f. for 20, 50, 100, and 200 nm, respectively. This shortening of the scattering time is accompanied to a respective increase in the free electron density of 1.50, 3.30, 1.50, and 20.50 $\times 10^{17}$(cm^{-3}). The increase in the free electron density is expected because the thicker the metal slab, the more electrons that are available for conduction (indium have three valence electrons). Moreover, a pronounced effect on the electron drifts mobility and plasmon frequency may be observed from Table 2. The drift mobility decreases from 12.58 to 8.38, 6.81, and 5.76 cm^2/Vs as the In thickness increases from 20 to 50, 100, and 200 nm, respectively. The plasmon frequency also continually increased with increasing In layer thickness. It reaches a value of 2.08 GHz when the In slab thickness was 200 nm. The increase in the plasmon frequency in accordance with the relation $w_{pe} = \sqrt{4\pi ne^2/m^*}$ should be

Table 2 The computed parameters of the plasmonic interactions in the Ga_2S_3/In/Ga_2S_3 films

d(nm)	20				50				100				200			
i	1	2	3	4	1	2	3	4	1	2	3	4	1	2	3	4
$\tau_i(fs)$	1.20	1.00	1.00	0.60	0.80	0.80	0.80	0.55	0.65	0.65	0.65	0.60	0.55	0.55	0.50	0.30
$w_{ei}(\times 10^{15} Hz)$	3.00	3.20	4.70	6.00	2.50	3.50	5.00	6.40	2.90	3.25	4.90	6.50	2.20	3.50	4.60	5.40
$n\ (\times 10^{17} cm^{-3})$	1.50	1.70	4.50	37.00	3.30	7.10	26.00	35.00	10.50	10.50	28.00	28.00	20.50	20.50	20.50	20.50
$\mu(cm^2/Vs)$	12.58	10.48	10.48	6.29	8.38	8.38	7.34	5.76	6.81	6.81	6.81	6.28	5.76	5.76	5.24	3.14
$w_{pi}(GHz)$	0.56	0.59	0.97	2.79	0.83	1.18	2.29	2.55	1.49	1.49	2.43	2.43	2.08	2.08	2.29	2.29

assigned to the increase in the free electron density with increasing In slab thickness. The plasmon frequency indicates wide tunability in the performance of the Ga_2S_3/In/Ga_2S_3 interfaces when employed for microwave applications. The increase in the plasmon frequency with increasing the nanosandwiched metal slab thickness was also observed for the the ZnS/Ag/ZnS thin films [22]. The behavior was also assigned to the increase in the free electron density that is associated with increasing Ag layer thickness. In addition, the ZnS/Ag/ZnS films were shown to be ideal for the designing of broad band filters. The suitability of this design raised from the enhancement of the extinction coefficient and lowering of refractive index in the infrared region which is accepted to be useful for improving the performance of the broad band filters [22]. In addition, the increase of the Au film thickness from 26 to 40 nm in the ZnS/Au/ZnS trilayer decreased the energy band gaps from 4.95 to 4.90 eV. That reduction in the energy band gap was also assigned to the increase in the free carrier density upon Au thickness increasing [4]. The so-called many-body effects are reported to cause upward shifting of the valence band and downward shifting of the conduction band resulting in the band gap shrinkage [23].

In relative to our investigation, we should consider that the In is a free electron metal, with three electrons per atom in the metallic Fermi surface. The free electrons form a plasma that makes the indium opaque and highly reflective below the plasma frequency. On the upper and lower sides of In, the existence of the Ga_2S_3 with energy band gaps of 3.68, 2.98, and 2.51 eV will allow the absorbance of photons with energies above the energy band gaps, causing the generation of electron hole pairs. In addition to the generation process, the high energy of photons above the energy band gap which is an external time dependent electric field displaces the Ga^{+3} and S^{-2} ions producing induced dipoles. This explains the increase in the dielectric constant in the high frequency range above 740 THz (3.9–3.0 eV). Similarly, the increase in the dielectric constant in the frequency range of 640–470 THz (2.6–1.9 eV) can be, probably, assigned to the increase in the interfacial polarization between the Ga^{+3}, In^{+3}, and S^{-2} ion cores. During the growth process, the interfaces between the glassy regions and the randomly distributed crystallites which are having different dielectric constants and conductivities could be the origin of charge accumulation and interfacial polarization [24, 25].

Conclusions

In this systematic work, we have observed that the indium nanosandwiching between two Ga_2S_3 layers enhances the optical absorbability, redshifts the energy band gap, and increases the dielectric constant of the gallium sulfide thin films. The indium film thickness strongly attenuates the optical properties of the Ga_2S_3 without altering the structure. For thin layers of In slabs (20 nm), the Ga_2S_3/In/Ga_2S_3 is very attractive for optoelectronic applications near ultraviolet regions. On the other hand, increasing the thickness to 200 nm seems to be more suitable for infrared optoelectronic application.

Acknowledgments The authors would like to thank the scientific research council of Arab American University (SRC-AAUJ) at Palestine for the financial support. The work was supported by the SRC-AAUJ under the code (2016–2017 Cycle I). This project was also supported by the Deanship of Scientific Research (DSR), King Abdulaziz University, Jaddah. The authors, therefore, acknowledge with thanks the DSR technical and financial support.

References

1. Kavei G, Nikbin S (2015) Substrate temperature effect on the nanoscale multilayer ZnS/Ag/ZnS for heat mirror application. Mater Sci-Poland 33(4):760–766
2. Peres L, Bou A, Barakel D, Torchio P (2016) ZnS|Ag|TiO 2 multilayer electrodes with broadband transparency for thin film solar cells. RSC Adv 6(66):61057–61063
3. Zolanvari A, Norouzi R, Sadeghi H (2015) Optical properties of ZnS/Ag/ZnS transparent conductive sandwich structures investigated by spectroscopic ellipsometry. J Mater Sci Mater Electron 26(6): 4085–4090
4. Wang C, Li Q, Wang J, Zhang L, Zhao F, Dong F (2016) High quality ZnS/Au/ZnS transparent conductive tri-layer films deposited by pulsed laser deposition. Opt Spectrosc 121(1):68–71
5. Hira T, Homma T, Uchiyama T, Kuwamura K, Kihara Y, Saiki T (2015) All-optical switching of localized surface plasmon

resonance in single gold nanosandwich using GeSbTe film as an active medium. Appl Phys Lett 106(3):031105
6. Malasi A, Taz H, Ehrsam M, Goodwin J, Garcia H, Kalyanaraman R (2016) Enhanced and tunable optical quantum efficiencies from plasmon bandwidth engineering in bimetallic CoAg nanoparticles. APL Photonics 1(7):076101
7. Cui W, Chu Sh, Yu Li, Liang Y, Peng W (2016) Extraordinary optical transmission performances of nanosandwiched grating for wideband multi-function integration. Plasmonics 1–8
8. Alharbi SR, Qasrawi AF (2016) Dielectric dispersion in Ga2S3 thin films. Plasmonics. doi:10.1007/s11468-016-0357-4
9. Madelung O (2012) Semiconductors: data handbook. Springer Science & Business Media
10. Barnier S, Guittard M, Palazzi M, Massot M, Julien C (1992) Raman and infrared studies of the structure of gallium sulphide based glasses. Mater Sci Eng B 14(4):413–417
11. Arora AK, Rajalakshmi M, Ravindran TR, Sivasubramanian V (2007) Raman spectroscopy of optical phonon confinement in nanostructured materials. J Raman Spectrosc 38(6):604–617
12. Liu HF, Antwi KKA, Chua CS, Huang J, Chua SJ, Chi DZ (2014) Epitaxial synthesis, band offset, and photoelectrochemical properties of cubic Ga2S3 thin films on GaAs (111) substrates. ECS Solid State Lett 3(11):P131–P135
13. Aydinli A, Gasanly NM, Gökşen K (2000) Donor–acceptor pair recombination in gallium sulfide. J Appl Phys 88(12):7144–7149
14. Pistor P, Álvarez JMM, León M, di Michiel M, Schorr S, Klenk R, Lehmann S (2016) Structure reinvestigation of α-, β- and γ-In2S3. Acta Crystallogr Sect B: Struct Sci Cryst Eng Mater 72(3):410–415
15. Bouabid K, Ihlal A, Outzourhit A, Ameziane EL (2004) Structural and optical properties of In2S3 thin films prepared by flash evaporation. Act Passive Electron Compon 27(4):207–214
16. Zhao Z, Cao Y, Yi J, He X, Ma C, Qiu J (2012) Band-edge electronic structure of β-In2S3: the role of s or p orbitals of atoms at different lattice positions. ChemPhysChem 13(6): 1551–1556
17. Zhang M, Jiang X, Zhou L, Guo G (2013) Two phases of Ga2S3: promising infrared second-order nonlinear optical materials with very high laser induced damage thresholds. J Mater Chem C 1(31):4754–4760
18. Seeburrun N, Archibong EF, Ramasami P (2008) Structures and electron detachment energies of Ga2S3 and Ga3S2. Chem Phys Lett 467(1):23–27
19. Oh G, Jeon J, Lee KS, Kyu Kim E (2016) Work function modification of tungsten-doped indium oxides deposited by the co-sputtering method. J Nanosci Nanotechnol 16(5):5109–5113
20. Sze SM, Ng KK (2006) Physics of semiconductor devices, 3rd edn. Wiley, New Jersey
21. Xue Z, Liu X, Lv Y et al (2015) Low-work-function, ITO-free transparent cathodes for inverted polymer solar cells. ACS Appl Mater Interfaces 7(36):19960–19965
22. Zhao P, Su W, Wang R, Xu X, Zhang F (2009) Properties of thin silver films with different thickness. Physica E: Low-Dimens Syst Nanostruct 41(3):387–390
23. Indluru A, Alford TL (2009) Effect of Ag thickness on electrical transport and optical properties of indium tin oxide–Ag–indium tin oxide multilayers. J Appl Phys 105(12):123528
24. Ho C, Chen H (2014) Optically decomposed near-band-edge structure and excitonic transitions in Ga2S3. Sci Report 4: 6143
25. Vaish R, Varma KBR (2011) Electrical relaxation and transport in 0.5 Cs2 O-0.5 Li 2O-3B2O 3 glasses. IEEE Trans Dielectr Electr Insul 18(1):155–161